GANAPATY ALAGUMUTHU
VELLAISAMY
VEERAPUTHIRAN
RAMASWAMY
VENKATARAMAN

Chemistry Research Centre,
Sri Paramakalyani College,
Tamilnadu, India

SCIENTIFIC PAPER

UDC 66.081.3:58:615.916

DOI: 10.2298/HEMIND100712052A

FLUORIDE SORPTION USING *Cynodon dactylon*-BASED ACTIVATED CARBON

This study deals with the application of Cynodon dactylon-based thermally activated carbon for fluoride toxicity. The batch adsorption technique was followed at neutral pH as a function of contact time, adsorbent dose, adsorbate concentration, temperature and the effect of co-anions. The data indicate that the prepared adsorbent surface sites are heterogeneous in nature and that fits into a heterogeneous site-binding model. The present system followed the Redlich–Peterson isotherm as well as the Langmuir adsorption isotherm model. Lagergren pseudo-first-order, pseudo-second-order, intra particle diffusion and Elovich kinetics were modeled to describe the adsorption rate of fluoride, and determined as this scheme followed pseudo-second-order kinetics. The calculated enthalpy change, $\Delta H°$, and entropy change, $\Delta S°$, for the adsorption process were 8.725 kJ/mol and 0.033 J/mol K, respectively, and showed endothermic experience. Instrumental analysis of XRD, FTIR and SEM gives an idea about the fluoride binding ability of adsorbent.

The high fluoride level in drinking water has become a critical health hazard of this century as it induces intense impact on human health including skeletal and dental fluorosis [1]. Though fluoride is an essential constituent for both humans and animals, it can be either beneficial or detrimental to human health depending on the level of fluoride in drinking water [2]. In India, this problem is common in places such as Andhra Pradesh, Tamilnadu, Karnataka, Kerala, Rajasthan, Gujarat, Uttar Pradesh, Punjab, Orissa and Jammu and Kashmir [3]. The free fluoride level in drinking water was identified at 3.02 mg/L in Kadayam block of Tamilnadu [4]. A fluoride survey in Nilakottai block of Tamilnadu showed a positive correlation between the prevalence of dental fluorosis in children and levels of fluoride in portable water is 3.24 mg/L [5].

Adsorption is one of the significant techniques in which fluoride is adsorbed onto a membrane, or a fixed bed packed with resin or other mineral particles. Many natural and low cost materials such as red mud [6,7], zirconium impregnated coconut shell carbon [8], cashew nut shell carbon [9], ground nut shell carbon [10] and clays [11] have been used as adsorbents for fluoride removal from drinking water. Recently, amorphous alumina supported on carbon nanotubes [12], aligned carbon nanotubes [13], ion exchange polymeric fiber [14], and an ion exchanger based on a double hydrous oxide of Al and Fe ($Fe_2O_3Al_2O_3{\times}H_2O$) [15] have been assayed for removing fluoride from drinking water as well as industrial wastewater.

Thus, it is important to develop or find cheaper adsorbents for fluoride removal from water that have greater fluoride adsorption capacities like the above said adsorbents. This paper concentrates on investigating low cost materials for fluoride sorption which can effectively remove fluoride from aqueous solutions at a relatively low level. The novel adsorbent obtained by burning, carbonization and thermal activation of the *Cynodon dactylon*, possesses an appreciable defluoridation efficiency. The thermally activated carbon should have a high surface area and strong sorption capacity towards various sorbates [16]. This adsorbent is abundantly available in all dry and wet lands in huge amount. We report here the results of defluoridation studies using *Cynodon dactylon*. This study leads to the assumption that fluoride deposition occurs by the forces of adsorption over the surface of the activated carbon and this was characterized by the surface morphological studies of the adsorbent material. In addition, the dynamics and kinetics of the adsorption process are discussed.

EXPERIMENTAL

Adsorbent preparation

The *Cynodon dactylon* sample, common name Bermuda grass, was collected from nearby Western Ghats area and washed thoroughly with double distilled water. The material was then kept aside for shadow dry and then dried at 378–383 K for 24 h. It was washed with doubly distilled water in order to remove the free acid and dried at the same temperature for 3 h. Later, the dried adsorbent was thermally activated in Muffle furnace at 1073 K (here we avoid acid treatment for charring). The resulting product was cooled to room temperature and sieved to the desired particle sizes, namely, <53, 53–106, 106–150, 150–225 and 225–305 mesh. Finally, the product was stored in vacuum desiccators until required.

Sorption experiments

The sorption isotherm and kinetics experiments were performed by batch adsorption experiments and were carried out by mixing 1.25 g (obtained by the study effect of adsorbent dose) of sorbent with 100 mL of sodium fluoride containing 3 mg/L as initial fluoride

Corresponding author: G. Alagumuthu, Chemistry Research Centre, Sri Paramakalyani College, Alwarkurichi-627412, Tamilnadu, India.
E-mail: liviveera@yahoo.co.in
Paper received: 12 July, 2010
Paper accepted: 16 September, 2010

concentration. The mixture was agitated in a thermostatic shaker at a speed of 250 rpm at room temperature. The defluoridation studies were conducted for the optimization of various experimental conditions like contact time, initial fluoride concentration, adsorbent dose, particle size and influence of co-ions with fixed dosage. The reagents used in this present study are of analytical grade. A fluoride ion stock solution (100 mg/L) was prepared and other fluoride test solutions were prepared by subsequent dilution of the stock solution. All the experiments were carried out at room temperature. Fluoride ion concentration was measured with a specific ion selective electrode by use of total ionic strength adjustment buffer II (TISAB II) solution to maintain pH 5–5.5 and to eliminate the interference effect of complexing ions [9]. The pH of the samples was also measured by Orion ion selective equipment. All other water quality parameters were analyzed by using standard methods [17]. The kinetic studies of the sorbent were carried out in a temperature controlled mechanical shaker. The effect of different initial fluoride concentrations, viz., 2, 4, 6, 8 and 10 mg/L at four different temperatures, viz., 303, 313, 323 and 333 K on sorption rate were studied by keeping the mass of sorbent as 1.25 g and volume of solution as 100 mL in neutral pH.

The fluoride concentration retained in the adsorbent phase, q_e (mg/g), was calculated according to [18]:

$$q_e = \frac{c_0 - c_e}{W} \tag{1}$$

where c_0 and c_e are the initial and residual concentration at equilibrium (mg/L), respectively, of fluoride in solution; and W is the weight (g) of the adsorbent.

Characterization of sorbents

The physicochemical properties of the activated carbon are shown in Table 1. The X-ray diffraction (XRD) pattern of adsorbent was obtained using a Bruker AXS D8 Advance, Inst ID: OCPL/ARD/26-002 X-ray diffractometer. Fourier transform infrared (FTIR) spectra were recorded using a Nicolet 6700, Thermo Electronic Corporation, USA, spectrophotometer. The scanning electron microscopy (SEM) analysis performed using a Philips XL-20 electron microscope. Computations were made using a Microcal Origin (Version 6.0) software. The accuracies of fits are discussed using regression correlation coefficient, r, and chi-square analysis (SSE). The chi-square statistic test is basically the sum of the square of the difference between the experimental data and data obtained by calculating from the models, with each squared difference divided by the corresponding data obtained by calculating from the models. The equivalent mathematical statement [19] is:

$$\chi^2 = \Sigma \frac{(q_e - q_e, m)^2}{q_e, m} \tag{2}$$

where q_e,m is equilibrium capacity obtained by calculating from the model (mg/g), and q_e is experimental data of the equilibrium capacity (mg/g).

Theory of isotherm and kinetic modeling

The abilities of four widely used isotherms, the theoretical Langmuir, empirical Freundlich, Temkin and Redlich–Peterson isotherms, to model the adsorption equilibrium data were examined. To express the mechanism of fluoride adsorption onto the surface of adsorbent, the kinetic models pseudo-first-order, pseudo-second-order, intra particle diffusion, Elovich models and thermodynamic parameters are used to analyze the present adsorption data to determine the related kinetic parameters.

The Langmuir adsorption isotherm [20], perhaps the best known of all isotherms, is often applied in solid/liquid systems to describe the saturated monolayer adsorption. It can be represented as:

$$q_e = \frac{q_m K_a c_e}{1 + K_a c_e} \tag{3}$$

where q_m is q_e for a complete monolayer (mg/g); K_a is the adsorption equilibrium constant (L/mg). To evaluate the adsorption capacity for a particular range of adsorbate concentration, the aforementioned equation (Eq. (3)) can be used in the following linear form:

$$\frac{c_e}{q_e} = \frac{1}{q_m} c_e + \frac{1}{K_a q_m} \tag{4}$$

The constants q_m and K_a can be determined by Eq. (4) from the slope of the linear plot of c_e/q_e versus c_e.

Table 1. Texture properties of the Cynodon dactylon based activated carbon

No.	Physical parameter	Value
1	Surface area, m^2/g	7.3
2	Density, g/cm^3	1.13
2	Particle size, μm	>53
3	Specific volume, dm^3/kg	0.885
4	Moisture, mass %	20.32
5	Ash content, mass %	39.44

Freundlich adsorption isotherm [21], based on adsorption on heterogeneous surface is the earliest known relationship describing the adsorption equilibrium and is given by:

$$q_e = K_F c_e^{\frac{1}{n}} \quad (5)$$

where K_F and $1/n$ are empirical constants, indicating the adsorption capacity and adsorption intensity, respectively. Equation (5) may be converted to a linear form by taking logarithms:

$$\log q_e = \log K_F + \frac{1}{n} \log c_e \quad (6)$$

The plot of log q_e *versus* log c_e of Eq. (6) should result in a straight line. From the slope and intercept of the plot, the values for n and K_F can be obtained.

The Temkin isotherm [22], the simple form of an adsorption isotherm model, has been developed considering the chemisorption of an adsorbate onto the adsorbent, is represented as:

$$q_e = a + b \log c_e \quad (7)$$

where q_e and c_e have the same meaning as noted previously and the other parameters are called the Temkin constants. The plot of q_e *versus* log c_e will generate a straight line. The Temkin constants a and b can be calculated from the slope and intercept of the linear plot.

The Redlich–Peterson isotherm [23] contains three parameters and incorporates the features of the Langmuir and Freundlich isotherms. It can be described as follows:

$$q_e = \frac{A c_e}{1 + B c_e^g} \quad (8)$$

Equation (8) can be converted to a linear form by taking natural logarithms:

$$\ln\left(A \frac{c_e}{q_e} - 1\right) = g \ln c_e + \ln B \quad (9)$$

The three isotherm constants, A, B, and g ($0 < g < < 1$), can be evaluated from the linear plot represented by Eq. (9) using a trial and error optimization method [24].

The pseudo-first-order kinetic model, the Lagergren rate equation, has been the most widely used rate equation for assigning the adsorption of an adsorbate from a liquid phase since 1898 [25]. The linear form of the pseudo-first-order equation is represented as:

$$\log(q_e - q_t) = \log q_e - \frac{k_L}{2.303} t \quad (10)$$

where q_t is the adsorption capacity (mg/g) at time t; k_L (min^{-1}) is the rate constant of the pseudo-first-order adsorption reaction. The plot of log (q_e–q_t) *versus* t should give a straight line from which k_L and q_e can be calculated from the slope and intercept of the plot, respectively.

The pseudo-second-order model was developed by Ho and McKay [26] to describe the adsorption of some metal ion onto the adsorbent. The linear form of the pseudo-second-order adsorption kinetic rate equation is expressed as:

$$\frac{t}{q_t} = \frac{1}{k_2 q_e^2} + \frac{t}{q_e} \quad (11)$$

where q_e and q_t have the same meaning as mentioned previously, and k_2 is the rate constant for the pseudo-second-order adsorption reaction (g/mg min^{-1}). The value of q_e and the pseudo-second-order rate constant, k_2, can be calculated from the slope and intercept of the straight line obtained from the plot of t/q_t *versus* t. The initial adsorption rate can be obtained as q_t/t when t approaches zero:

$$h_0 = k_2 q_e^2 \quad (12)$$

where h_0 is the initial adsorption rate (mg/g min^{-1}).

In intraparticle diffusion model [27], the adsorbate moves from the solution phase to the surface of the adsorbent particles in several steps. The overall adsorption process may be controlled by one or more steps (*e.g.*, film or external diffusion, pore diffusion, surface diffusion and adsorption on the pore surface, or a combination of more than one step). In a rapidly stirred batch process of adsorption, the diffusive mass transfer can be related by an obvious diffusion coefficient, which will fit experimental adsorption rate data. Normally, a process is diffusion-controlled if its rate is dependent on the rate at which components diffuse toward each other. The possibility of intraparticle diffusion was explored using the intraparticle diffusion model:

$$q_t = k_{id} t^{1/2} + C \quad (13)$$

where k_{id} is the intraparticle (pore) diffusion rate constant (mg/g $\text{min}^{-0.5}$) and C is the intercept that gives an idea about the thickness of the boundary layer. The larger the value of C, the greater the boundary-layer effect.

Elovich model [28], which is based on chemisorption phenomena, is expressed as in a linear equation [29] as:

$$q_t = \beta \ln \alpha\beta + \frac{1}{\beta} \ln t \quad (14)$$

where α is the initial sorption rate (mg/g min^{-1}) and β is the desorption constant (g/mg) during the experiment. From the intercept and slope of the straight line obtained from the plot of q_t *versus* ln t, the values for α and β were calculated.

Thermodynamic parameters. The thermodynamic parameters for the adsorption process in solution have been calculated using the following standard thermodynamic relations:

$$\Delta G^{\ominus} = -RT\ln K_0 \quad (15)$$

where $\Delta G^{\ominus}$ is the standard free energy change (kJ/mol), T is the temperature (K) and R is universal constant (8.314 J mol^{-1} K^{-1}). The sorption distribution coefficient, K_0, for the sorption reaction was determined from the slope of the plot ln (q_e/c_e) against c_e at different temperatures and extrapolating to zero c_e [10].

The sorption distribution coefficient may be expressed in terms of $\Delta H^{\ominus}$ and $\Delta S^{\ominus}$ as a function of temperature:

$$\ln K_0 = \Delta H^{\ominus}/RT + \Delta S^{\ominus}/R \quad (16)$$

where $\Delta H^{\ominus}$ is the standard enthalpy change (kJ/mol) and $\Delta S^{\ominus}$ is the standard entropy change (kJ mol^{-1} K^{-1}). The values of $\Delta H^{\ominus}$ and $\Delta S^{\ominus}$ can be obtained from the slope and intercept of a plot of ln K_0 against $1/T$ [30].

RESULTS AND DISCUSSION

Effect of contact time and initial fluoride concentration

Contact time plays a very important role in adsorption dynamics. The effect of contact time on adsorption of fluoride onto *Cynodon dactylon* is shown in Figure 1. Batch adsorption studies using the concentrations 2.0, 3.0, 4.0, 6.0, 8.0 and 10.0 mg/L of fluoride solution and with 1.25 g of the adsorbent were carried out at 303 K as a function of time to evaluate the defluoridation and adsorption rate constants. The adsorption of fluoride increases with time and gradually attains equilibrium after 105 min. From Figure 1, the time to reach equilibrium conditions appears to be independent of initial fluoride concentrations. Therefore 105 min was fixed as minimum contact time for the maximum defluoridation of the sorbent. The adsorption of fluoride decreased from 84 to 51% by increasing fluoride concentration from 2.0 to 10.0 mg/L. Further, it was observed that the removal curves are smooth and continuous, indicating the possibility of the formation of monolayer coverage of the fluoride ion at the interface of adsorbent.

Effect of particle size

The defluoridation experiments were conducted using *Cynodon dactylon* with five different particle sizes, viz. >53, 53–106, 106–150, 150–225 and 225–303 μm. As the adsorption process is a surface phenomenon, the defluoridation efficiency of the sample with 53 μm registered high defluoridation efficiency due to larger surface area. The percentages of fluoride removal by the sample with different particle sizes are studied. Hence, the material with particle size of 53 μm has been chosen for further experiments. Higher percentage of adsorption by *Cynodon dactylon* with smaller particle size is due to the availability of more specific surface area on the adsorbent surface.

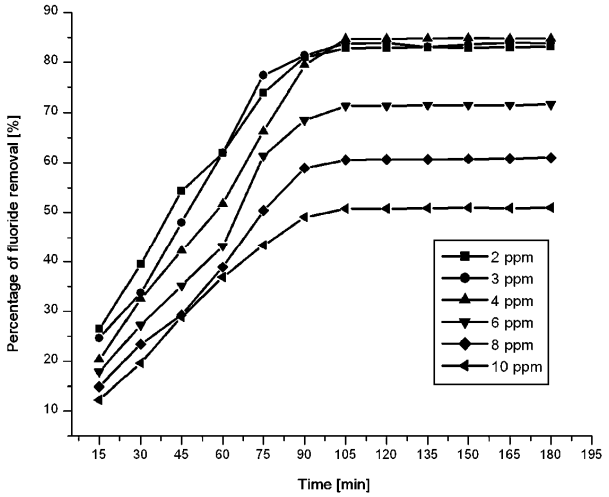

Figure 1. Percentage of fluoride adsorbed on Cynodon dactylon versus time for different initial fluoride concentrations.

Influence of adsorbent dose

The influence of varying concentrations of adsorbent on the adsorption of fluoride at neutral pH is shown in Figure 2. While increasing the adsorbent dose proportional removal observed for fluoride until some extent. After that, the curve lapse as flat indicating the higher fluoride adsorption occurs at 1.25 g and the followings remains constant. A distribution coefficient, K_D, reflects the binding ability of the surface for an element. The K_D values of a system mainly depend on pH and type of surface. The distribution coefficient values for fluoride and *Cynodon dactylon* at neutral pH were calculated [31] by means of:

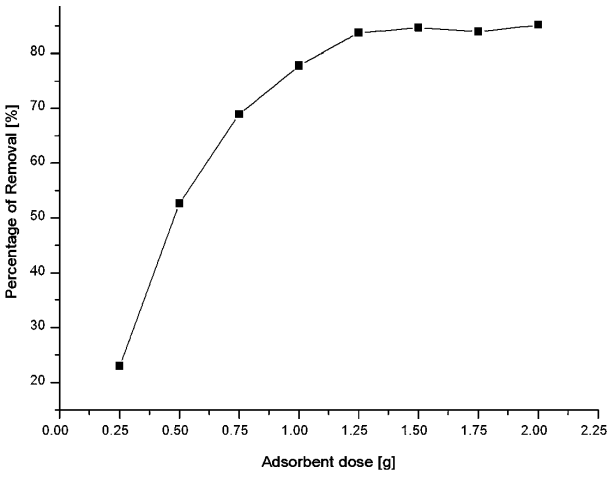

Figure 2. Variation of fluoride removal for different adsorbent dosages at constant temperature.

$$K_D = \frac{c_s}{c_w} \quad (15)$$

where c_s is the concentration of fluoride in the solid particles (mg/kg) and c_w is the concentration in water (mg/L). It is seen that the distribution coefficient increases with an increase in adsorbent concentration, indicating the heterogeneous surface of the adsorbent [18]. It is observed in Figure 3 that K_D increases with an increase in adsorbent concentration at constant pH. If the surface is homogeneous, the K_D values at a given pH should not change with adsorbent concentration. All the forthcoming experiments were carried out using a constant adsorbent dose of 1.25 g.

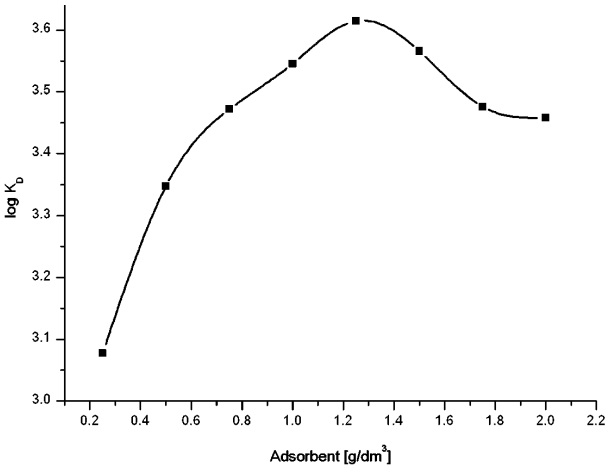

Figure 3. The relationship between distribution coefficient K_D with different adsorbent dosages.

Effect of interfering co-ions

The effects of coexisting anions such as sulfate, nitrate, chloride, and bicarbonate on fluoride adsorption by the *Cynodon dactylon* adsorbent were examined and the results are given in Figure 4. Chloride and nitrate ions did not noticeably interfere with fluoride removal even at a concentration of 500 mg/L, while sulfate ions began to show some adverse effects when the SO_4^{2-} concentration increased. However, bicarbonate showed great competitive adsorption with fluoride. The fluoride adsorption amount decreased quickly from 83.7 to 51.5% with the increase of bicarbonate concentration 0–300 mg/L, and then decreased slightly with further increase of bicarbonate concentration. This may be attributed to the competition of bicarbonate ions with the fluoride ions at the active site, on the surface of the sorbents. The selective nature of the fluoride by the sorbent depends on size, charge, polarizability, electronegativity difference, etc. The order of interference for fluoride removal observed as in the following order, $HCO_3^- > SO_4^{2-} > Cl^- \geq \geq NO_3^-$ for the adsorbent *Cynodon dactylon*. A similar trend was reported while studying zirconium impregnated cashew nut shell carbon as a sorbent for fluoride removal [9].

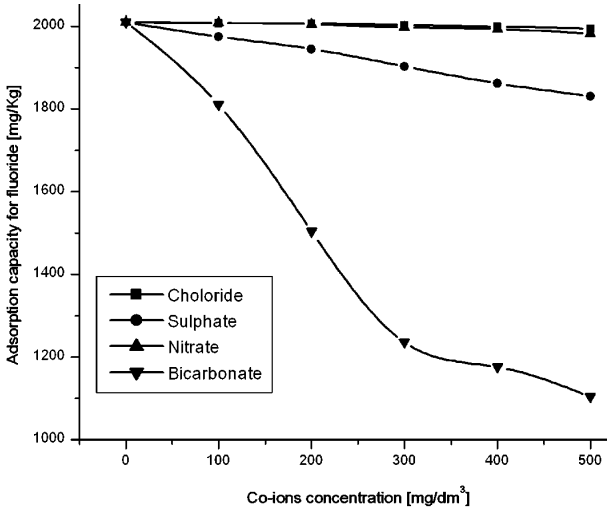

Figure 4. Interference of co-ions on defluoridation studies using Cynodon dactylon adsorbent.

Adsorption isotherms

The equilibrium data isotherm analysis for fluoride adsorption onto the *Cynodon dactylon* at pH 7.0 (±0.2) and at temperatures of 303, 313, 323 and 333 K are shown in Figures 5–8. Results indicate that the adsorbent has a high affinity for fluoride adsorption under these conditions. The equilibrium data has been analyzed by linear regression of isotherm model equations, viz. Langmuir (Figure 5), Freundlich (Figure 6), Temkin (Figure 7), and Redlich–Peterson (Figure 8). The related parameters obtained by calculation from the values of slopes and intercepts of the respective linear plots are shown in Table 2. The present data fit the Langmuir and Redlich–Peterson models (Figs. 5 and 8) well ($r^2 > 0.99$). The average monolayer adsorption capacity, q_m, obtained for *Cynodon dactylon* is 4.702 mg/g. The value

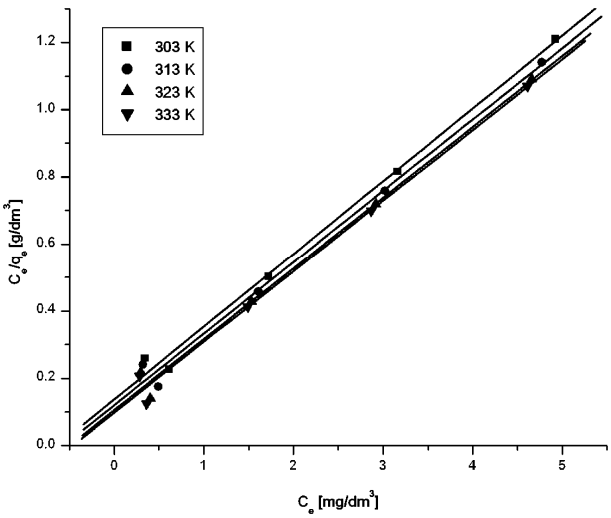

Figure 5. Langmuir isotherms obtained by using linear method for the adsorption of fluoride using activated adsorbent at various temperatures.

for the Redlich–Peterson constant A that is obtained as high (72.9–102.1 L/g) for the maximum optimized value for g (0.825–0.872), which indicates the high affinity of *Cynodon dactylon* for fluoride. These high g-values of the Redlich–Peterson model required to describe the best fit of the present data indicated that the adsorption of fluoride is due to the Langmuir monolayer surface adsorption. However, the Freundlich isotherm model, based on multilayer adsorption, describe the data fairly well (r in the 0.994–0.997 range). The Freundlich adsorption constants, K_F, obtained from the linear plot are between 3.0 and 3.4. The Freundlich coefficient, n, which should have values ranging from 1 to 10, is high (5.0–6.3), and that supports the favorable adsorption of fluoride onto the adsorbent. The linear plot for Temkin adsorption isotherm, which contains the features of chemisorption, relatively described the present isotherm adsorption data (r is in the 0.996–0.998 range). This indicated that the adsorption of fluoride onto the adsorbent might be happened by chemisorptions with physical forces (*i.e.*, physisorption followed by chemisorption). Hence, the order of isotherm equations obeyed by the present data is Redlich–Peterson > Langmuir > Freundlich > Temkin isotherm.

The effect of isotherm shape can be used to predict whether an adsorption system is "favourable" or "unfavourable". Tan *et al.* [32] used the essential features of the Langmuir isotherm which can be expressed in terms of a dimensionless constant separation factor or equilibrium parameter R_L, defined by the following relationship:

$$R_L = \frac{1}{1 + K_a c_0} \tag{16}$$

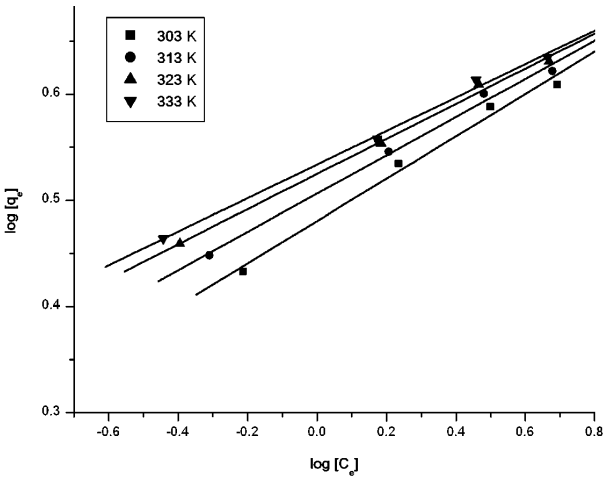

Figure 6. Plot of the Freundlich isotherm for fluoride adsorption on Cynodon dactylon.

where R_L is a dimensionless separation factor, c_0 the initial fluoride concentration (mg/L) and K_a the Langmuir constant (L/mg). The parameter R_L indicates the isotherm shape accordingly:

R_L	Type of Isotherm
>1	Unfavorable
1	Linear
between 0 and 1	Favorable
0	Irreversible

Table 2. Isotherm parameters obtained using the linear method for the adsorption of fluoride onto cynodon dactylon at different temperatures

Isotherm	Parameter	Temperature, K			
		303	313	323	333
Langmuir isotherm	q_m / mg g^{-1}	4.617	4.702	4.742	4.755
	K_a / dm^3 mg^{-1}	1.580	1.773	2.003	2.147
	r	0.999	0.998	0.998	0.999
	SSE	0.010	0.011	0.011	0.011
Freundlich isotherm	K_F / mg g^{-1}(dm^3 mg^{-1})$^{1/n}$	3.024	3.209	3.348	3.417
	1/n	0.199	0.180	0.165	0.158
	r	0.994	0.996	0.997	0.997
	SSE	0.016	0.010	0.008	0.008
Redlich-Peterson isotherm	g	0.825	0.847	0.863	0.872
	B / (dm^3 mg^{-1})^g	23.026	24.772	27.063	28.514
	A / dm^3 g^{-1}	72.971	83.361	94.985	102.114
	r	0.9998	0.9999	0.9999	0.9999
	SSE	0.013	0.008	0.008	0.009
Temkin isotherm	a / dm^3 g^{-1}	3.051	3.245	3.390	3.458
	b	1.528	1.419	1.332	1.288
	r	0.997	0.998	0.997	0.996
	SSE	0.079	0.064	0.068	0.077

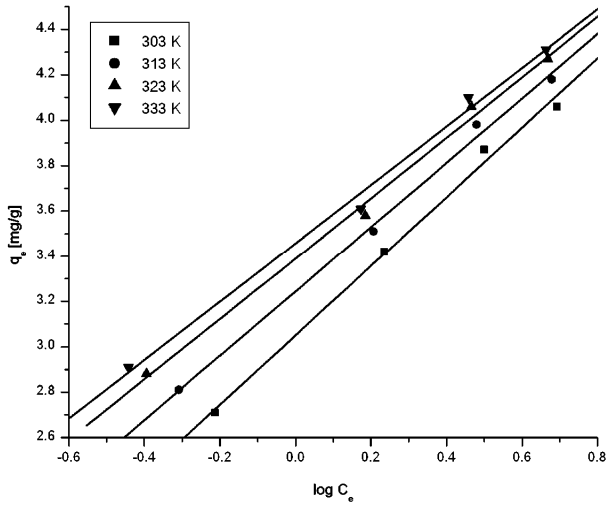

Figure 7. Adsorbent response to Temkin isotherm for fluoride removal at different temperatures.

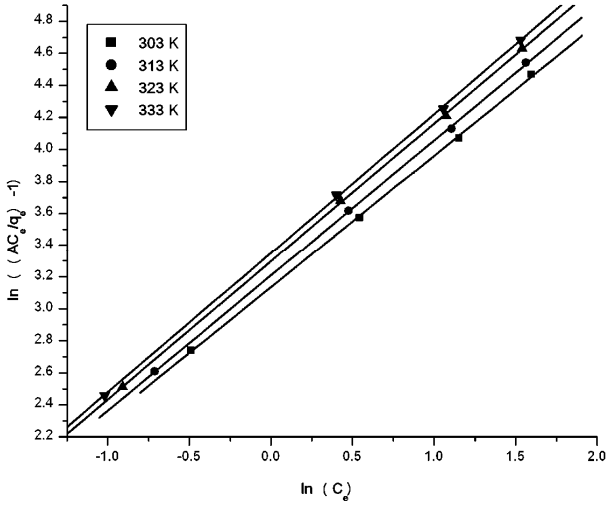

Figure 8. Redlich–Peterson isotherms for the sorption of fluoride ions by using Cynodon dactylon at various temperatures.

A figure with a relationship between R_L and c_0 is presented in Figure 9 to show the essential features of the Langmuir isotherm. Table 3 shows the values of R_L for *Cynodon dactylon* at different experimental temperatures. In this work, the R_L values calculated in the studied range of fluoride concentration are determined to be in the range of 0.044–0.24, which suggests favorable adsorption of fluoride onto the studied adsorbent, under the conditions used for the experiments.

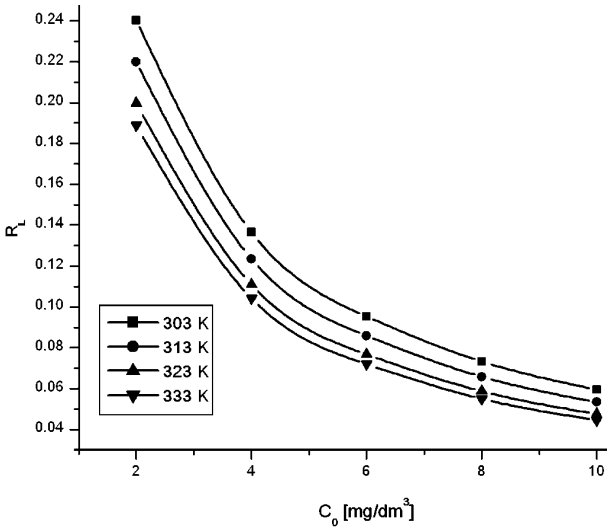

Figure 9. Separation factor R_L values verses initial fluoride concentration for various temperatures derived by Langmuir constants.

Adsorption kinetics

The results of the rate of fluoride adsorption on the *Cynodon dactylon* surface, as a function of the initial fluoride concentration, are shown in Figure 1. The fluoride adsorption was fast, up to 105 min, and then it became slow. The initial rapid adsorption was presumably due to active surface of the adsorbent. The slow adsorption in the later stage represents a gradual uptake of fluoride at the inner surface. These data were analyzed using kinetic equations, viz. pseudo-first-order (Figure 10), pseudo-second-order (Figure 11), intraparticle diffusion (Figure 12) and Elovich (Figure 13) models. The various related kinetic parameters, obtained by calculation from the slopes and intercepts of the plots are shown in Table 4. The Lagergren pseudo-first-order kinetic equation describes the kinetic data somewhat better (r is in the 0.89–0.94 range) for fluoride concentrations of 2.0–10.0 mg/L. The pseudo-second-order kinetic equation describes the present data best fit (r is in the 0.997–0.999 range) in the concentration range of fluoride used for the adsorption study (Figure 11). The equilibrium adsorption capacity, q_e, evaluated from the pseudo-second-order plot was determined to increase from 1.70 to

Table 3. R_L values at different temperatures, which were calculated using Langmuir constants

No.	Fluoride concetration mg/L	Temperature, K			
		303	313	323	333
1	2	0.240	0.220	0.200	0.189
2	4	0.137	0.124	0.111	0.104
3	6	0.095	0.086	0.077	0.072
4	8	0.073	0.066	0.059	0.055
5	10	0.060	0.053	0.048	0.044

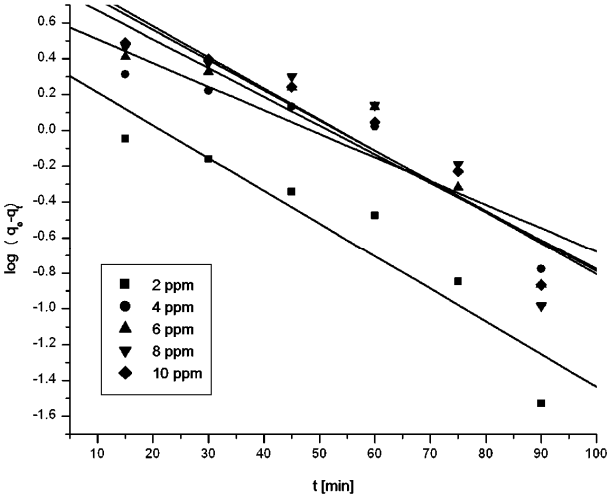

Figure 10. Pseudo-first-order kinetic fit for fluoride adsorption onto Cynodon dactylon at room temperature for different initial fluoride concentrations.

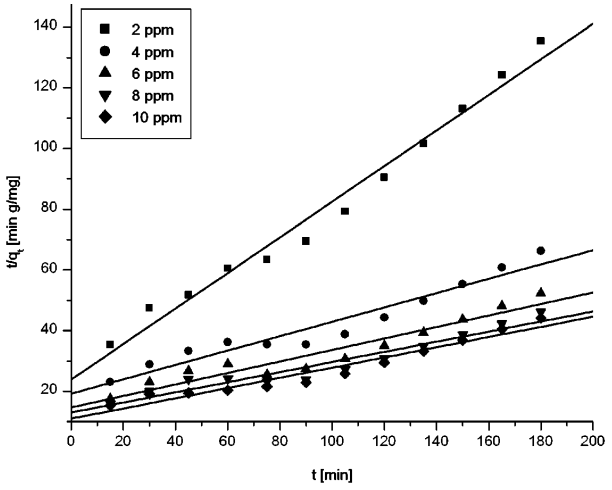

Figure 11. Pseudo-second-order kinetic fit for fluoride adsorption onto Cynodon dactylon at room temperature for different initial fluoride concentrations.

5.99 mg/g as the fluoride concentration increased from 2.0 to 10.0 mg/L, which suggests that the studied adsorbent should be a good adsorbent for scavenging fluoride from the contaminated water. The data were analyzed by the intraparticle diffusion kinetic equation and Figure 12 shows a plot of the mass of fluoride adsorbed per unit mass of adsorbent (q_t / mg g^{-1}) *versus* the square root of contact time ($t^{0.5}$ / min$^{0.5}$). It is indicated that the extrapolation of the first linear portion of the plots should not pass through the origin, so the adsorption rate of fluoride onto the adsorbent is not solely controlled by pore diffusion. Thus, the adsorption data indicated that the removal of fluoride from the aqueous phase onto the studied adsorbent was a rather complex process, maybe involving both boundary-layer diffusion and intraparticle diffusion. The increase of k_{id} (which denotes the average pore diffusion rate constant, mg/g min$^{0.5}$) with increasing concentration indicated a higher pore sorption possibility of fluoride onto the adsorbent at room temperature. From the Elovich model, the r values were found to be between 0.939 and 0.985 and fairly support to the formation of chemisorption followed by the physisorption. The present observation is consistent with the reported works [9].

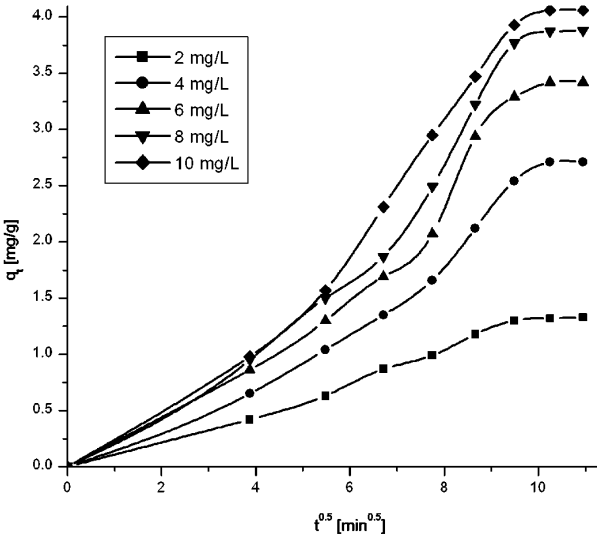

Figure 12. Plot for constant intra-particle diffusion at different temperatures.

Thermodynamic parameters

The effect of temperature is a major influence in the sorption process. Hence, the sorption of *Cynodon dactylon* was monitored at four different temperatures 303, 313, 323 and 333 K under the optimized condition and thermodynamic parameters, viz., standard free energy change, $\Delta G°$, standard enthalpy change, $\Delta H°$, and standard entropy change, $\Delta S°$, were calculated using Eqs. (15) and (16) and presented in Table 5 (Figure 14). The negative values of $\Delta G°$ indicated the spontaneity of the sorption reaction. The positive values of $\Delta H°$ indicated the endothermic nature of the sorption process. The positive value of $\Delta S°$ showed the increasing randomness at the solid/liquid interface during sorption of fluoride. The results showed an increase in adsorption capacity of fluoride with increasing temperature, which is presumably due to the control of the adsorption process by diffusion phenomenon. Thus, the results indicate the endothermic nature of the diffusion controlled adsorption process. They also indicate increased disorder in the system with changes in the hydration of adsorbing fluoride ions [33].

Instrumental analysis

The surface, morphology, and size distribution of the *Cynodon dactylon* adsorbent particles were observed by means of SEM, XRD and FTIR spectral analysis. The morphology of the fluoride treated adsorbent is shown

Table 4. Kinetic parameters for sorption of fluoride on cynodon dactylon for various fluoride concentrations at room temperature

Kinetic Model	Parameters	Initial fluoride concentration, mg/dm^3				
		2.0	4.0	6.0	8.0	10.0
Pseudo-first-order	k_L / min^{-1}	0.0422	0.0304	0.0370	0.0399	0.0388
	q_e / mg g^{-1}	2.4828	4.3607	6.7498	8.4744	7.9117
	r	0.9379	0.9213	0.9191	0.8971	0.9423
	SSE	0.0034	0.0028	0.0034	0.0043	0.0030
Pseudo-second-order	k_2 / g mg^{-1} min^{-1}	0.0144	0.0029	0.0024	0.0021	0.0026
	h / mg g^{-1} min^{-1}	0.0420	0.0521	0.0679	0.0771	0.0911
	r	0.9981	0.9973	0.9983	0.9993	0.9992
	SSE	0.0263	0.0196	0.0174	0.0147	0.0126
Intra-particle diffusion	k_p / mg g^{-1} min$^{-0.5}$	0.1323	0.2718	0.3484	0.3956	0.4176
	C	-0.0350	-0.2653	-0.3352	-0.3819	-0.3383
	r	0.9923	0.9805	0.9754	0.9777	0.9842
	SSE	0.0063	0.0206	0.0298	0.0321	0.0284
Elovich model	α / mg g^{-1} min^{-1}	0.0683	0.1057	0.1354	0.1534	0.1699
	β / g mg^{-1}	2.0408	0.9954	0.7480	0.6553	0.5998
	r	0.9849	0.9548	0.9398	0.9479	0.9778
	SSE	0.0431	0.1563	0.2429	0.2564	0.1788

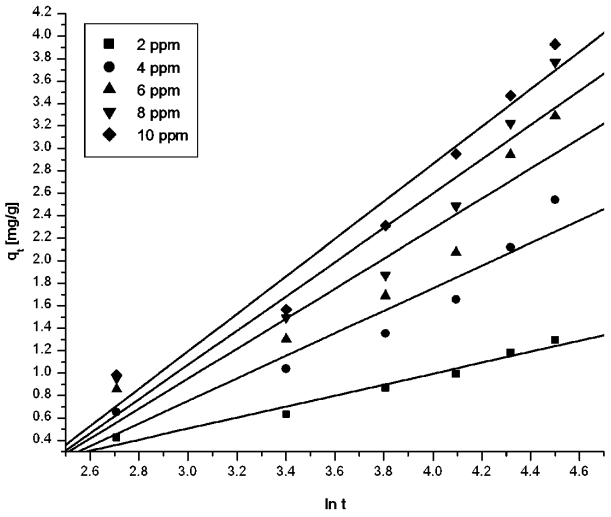

Figure 13. Linear plot for Elovich kinetic model for the temperatures 303, 313, 323 and 333 K.

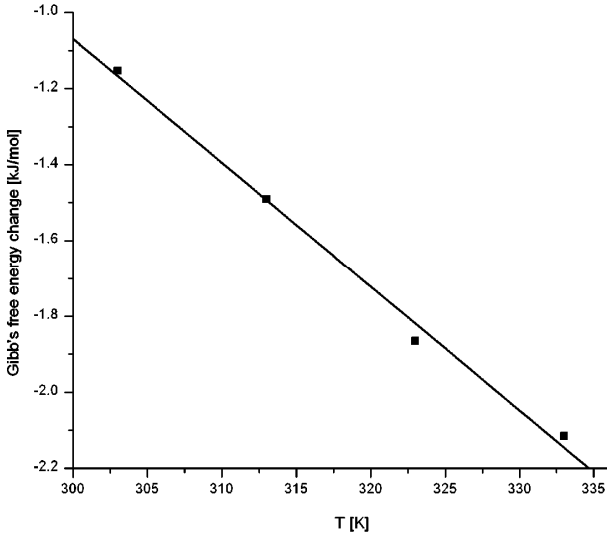

Figure 14. Plot of Gibbs free energy change ΔG°, versus temperature T.

in Figure 15, and it can be observed that the particles are presented as surface texture, flock and different levels of porous surface. The forms and sizes of the particles are very irregular after fluoride treatment. The XRD patterns of raw and fluoride treated material are given in Figure 16. The XRD data of the fluoride treated adsorbent provided evidence of considerable modification over the crystal cleavages by indicating some peak appearance at 2θ values of 29.38, 32.48 and 47.68° and intensity differences at 26.17 and 32.48°. A similar trend was observed by Shihabudeen *et al*. [34] in their study of fluoride removal from aqueous solutions. This shows the strong adsorption of fluoride on the surface of the adsorbent. The FTIR spectrum obtained (Figure 17) for the adsorbent displayed the following major bands: 3448.8 cm^{-1}: O–H stretch; 2924.18 cm^{-1}: C–H stretch; 1106.25 cm^{-1}: C–O stretch; 619.17 cm^{-1}: C–OH twist. It is reflecting the complex nature of adsorbent and shows significant band shifting and intensity changes due to fluoride sorption (Figures 17 and 18).

Field trial

The defluoridation efficiency of *Cynodon dactylon* in the field level was experienced with the sample collected from a near by fluoride-endemic villages. About 1.0 g of sorbent was added to 100 mL of fluoride water sample and the contents were shaken with constant time at room temperature. These results are presented in Tab-

Table 5. Thermodynamic parameters of fluoride sorption on Cynodon dactylon

No.	Thermodynamic Parameter	Temperature, K	Value
1	$\Delta G°$ / kJ mol^{-1}	303	–1.153
		313	–1.490
		323	–1.866
		333	–2.116
2	$\Delta H°$ / Kj mol^{-1}		8.725
3	$\Delta S°$/ J mol^{-1} K^{-1}		0.033

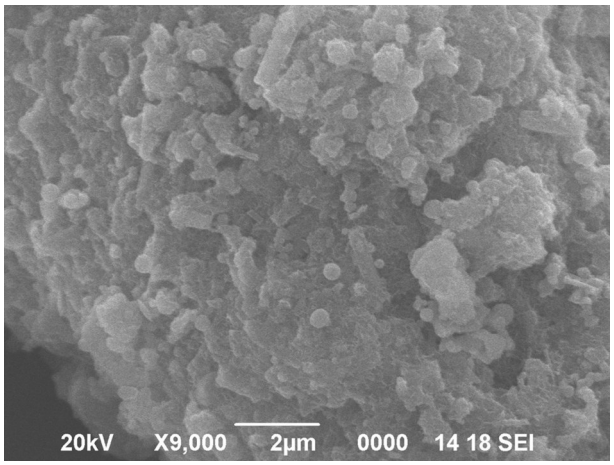

Figure 15. Scanning electron microscope view of fluoride--treated thermally activated Cycnodon dactylon adsorbent.

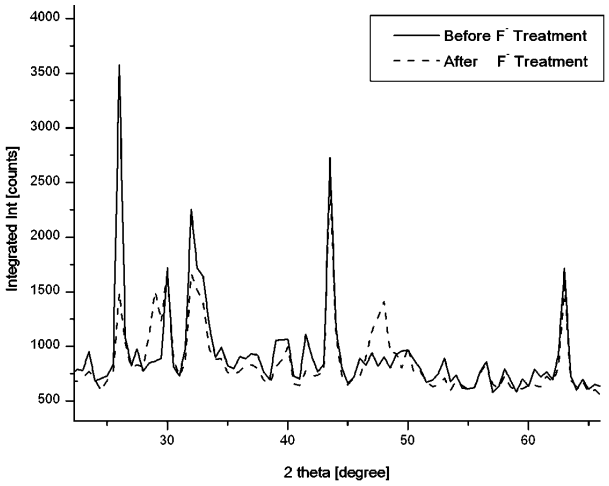

Figure 16. XRD pattern of pure and fluoride treated adsorbent.

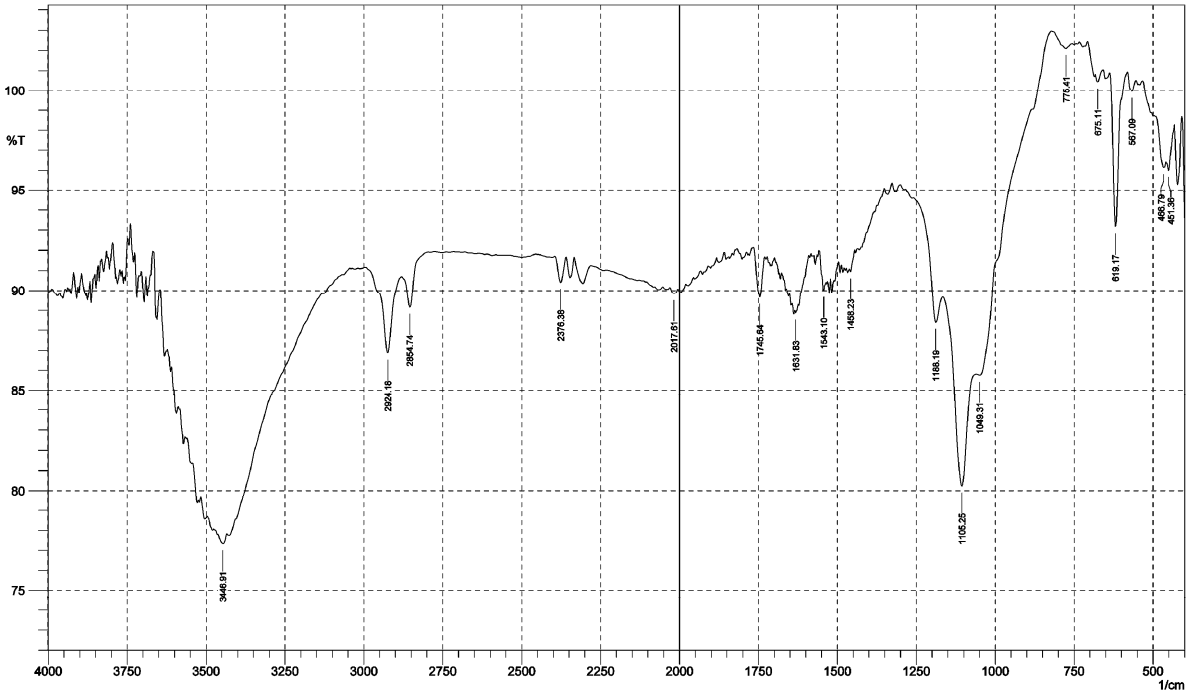

Figure 17. FTIR spectra of freshly prepared thermally activated adsorbent.

le 6. There is a significant reduction in the levels of other water quality parameters in addition to fluoride. It is evident from the result that the sorbent, *Cynodon dactylon* based adsorbent can be effectively employed for removing the fluoride from water.

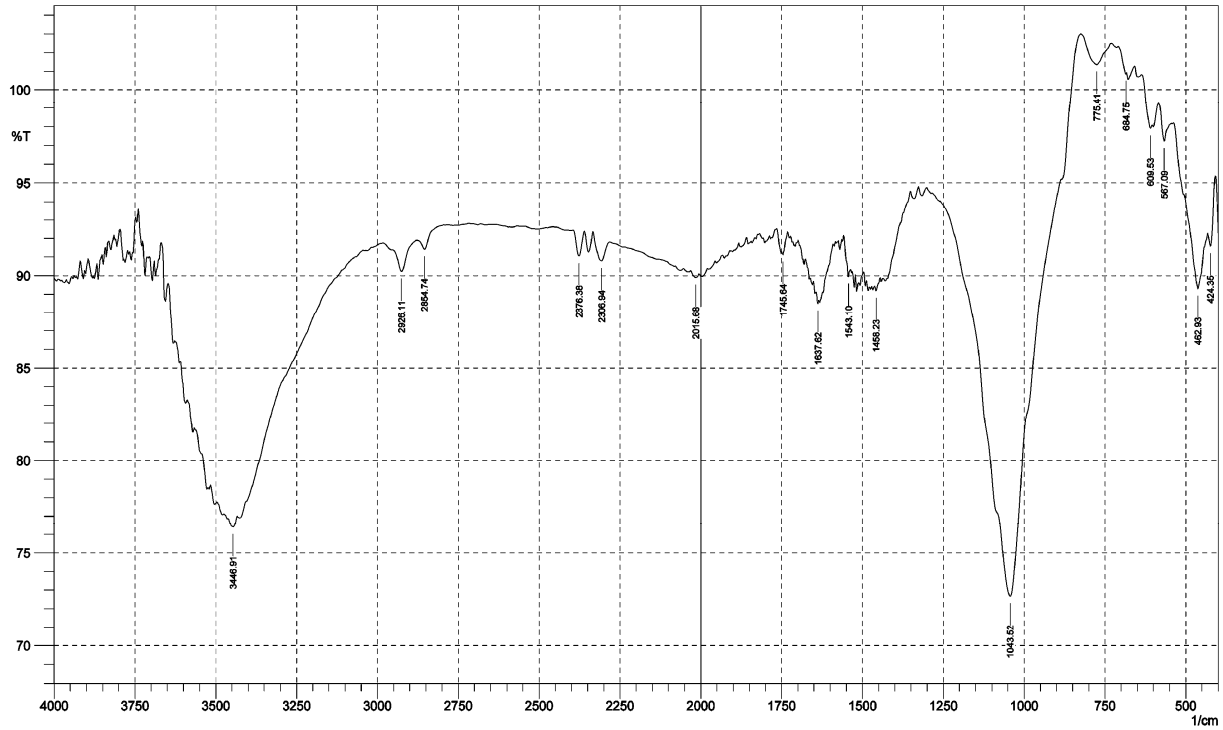

Figure 18. FTIR spectra of fluoride loaded adsorbent.

Table 6. Physico-chemical parameters of defluoridated drinking water from field

Water quality parameter	Before treatment	After treatment
Fluoride concentration, mg/L	3.14	1.03
pH	8.2	7.7
Electrical conductivity, μS/cm	361	217
Chloride concentration, mg/L	112	60
Total hardness, mg/L	394	212
Total alkalinity, mg/L	317	196

Regeneration study

Any adsorbent is economically viable if the adsorbent can be regenerated and reused in many cycles of operation. For checking the desorption capacity of the sorbent, the material was subjected to an adsorption at an initial fluoride concentration of 3 mg/L. The exhausted adsorbent was regenerated using 0–10% NaOH. At 2% NaOH concentration, *Cynodon dactylon* based adsorbent had desorbed up to the level of 67.4% of fluoride. To test the adsorption potential of regenerated adsorbent, two more cycles of adsorption–desorption studies were carried out by maintaining the initial conditions of the same. In third cycle, the adsorbent capacity has shown 19%. From the observations this adsorbent having somewhat reuse potential for fluoride removal.

CONCLUSION

The activated carbon was prepared successfully from *Cynodon dactylon* and studied in batch mode. Fluorides have been removed by the level of 83.77% while keeping 3.0 mg/L fluoride concentration and 1.25 g dosage of adsorbent at neutral pH. However, the presence of bicarbonate ions interfere the effective removal of fluoride. The sorption of fluoride using this adsorbent followed Redlich–Peterson isotherm as well as Langmuir isotherms and was found to be spontaneous and endothermic in nature. The rate of sorption followed the pseudo-second-order kinetic model and occurred through intraparticle diffusion. The used adsorbents could be regenerated by 67.4% using of 2% sodium hydroxide. Based on the above said descriptions, *Cynodon dactylon* bioadsorbent can be utilized to remove fluoride selectively from water.

Acknowledgement

Financial support for the project by the Department of Science and Technology (DST), Government of India, New Delhi, under the major research project is gratefully acknowledged.

REFERENCES

[1] S. Ayoob, A.K. Gupta, Fluoride in drinking water: a review on the status and stress effects, Crit. Rev. Environ. Sci. Technol. **36** (2006) 433–487.

[2] WHO, International Standards for Drinking Water, 3rd ed., Geneva, 2008.

[3] A.K. Susheela, Fluorosis management programme in India, Curr. Sci. **77** (10) (1999) 1250–1256.

[4] G. Alagumuthu, M. Rajan, Monitoring of fluoride concentration in ground water of Kadayam block of Tirunelveli district, India, Rasayan J. Chem. **4** (2008) 757––765.

[5] G. Viswanathan, A. Jaswanth, S. Gopalakrishnan, S. Siva ilango, Mapping of fluoride endemic areas and assessment of fluoride exposure, Sci. Total Environ. **407** (5) (2008) 1579–1587.

[6] Y. Cengeloglu, E. Kir, M. Ersoz, Removal of fluoride from aqueous solution by using red mud, Sep. Purif. Technol. **28** (2002) 81–86.

[7] A. Tor, N. Danaoglu, G. Arslan, Y. Cengeloglu, Removal of fluoride from water by using granular red mud: batch and column studies, J. Hazard. Mater. **164** (2009) 271–278.

[8] R.S. Sathish, N.S.R. Raju, G.S. Raju, G.N. Rao, K.A Kumar, C. Janardhana, Equilibrium and kinetics studies for fluoride adsorption from water on zirconium impregnated coconut shell carbon, Sep. Sci. Technol. **42** (2007) 769–788.

[9] G. Alagumuthu, M. Rajan, Equilibrium and kinetics of adsorption of fluoride onto zirconium impregnated cashew nut shell carbon, Chem. Eng. J. **158** (2010) 451–457.

[10] G. Alagumuthu, M. Rajan, Kinetic and equilibrium studies on fluoride removal by zirconium (IV) – impregnated ground nutshell carbon, Hem. Ind. **64** (4) (2010) 295–304.

[11] A. Tor, Removal of fluoride from an aqueous solution by using montmorillonite, Desalination **201** (2006) 267––276.

[12] Y.H. Li, S. Wang, A. Cao, D. Zhao, X. Zhang, J. Wei, C. Xu, Z. Luan, D. Ruan, J. Liang, D. Wu, B. Wei, Adsorption of fluoride from water by amorphous alumina supported on carbon nanotubes, Chem. Phys. Lett. **350** (2001) 412–416.

[13] Y.H. Li, S. Wang, X. Zhang, J. Wei, C. Xu, Z. Luan, D. Wu, adsorption of fluoride from water by aligned carbon nanotubes, Mater. Res. Bull. **38** (2003) 469–476.

[14] L. Ruixia, G. Jinlog, T. Hongxiao, Adsorption of fluoride, phosphate, and arsenate ions on a new type of ion exchange fiber, J. Colloid Interf. Sci. **248** (2002) 268––274.

[15] N.I. Chubar, V.F. Samanidou, V.S. Kouts, G.G. Gallios, V.A. Kanibolotsky, V.V. Strelko, I.Z. Zhuravlev, Adsorption of fluoride, chloride, bromide and bromate ions on a novel ion exchanger, J. Colloid Interf. Sci**. 291** (2005) 67–74.

[16] S. Sinha, K. Pandey, D. Mohan, K.P. Singh, Removal of fluoride from aqueous solutions by *Eichhornia crassipes* biomass and its carbonized form, Ind. Eng. Chem. Res. **42** (2003) 6911–6918.

[17] American Public Health Association, Standard methods for the examination of water and waste water, Washington DC, 14th Ed., 2007.

[18] M.G. Sujana, H.K. Pradhan, S. Anand, Studies on sorption of some geomaterials for fluoride removal from aqueous solutions, J. Hazard. Mater. **161** (2009) 120––125.

[19] Y.S. Ho, Selection of optimum sorption isotherm, Carbon **42** (2004) 2113–2130.

[20] I. Langmuir, The constitution and fundamental properties of solids and liquids, J. Am. Chem. Soc. **38** (1916) 2221–2295.

[21] H.M.F. Freundlich, Über die adsorption in lösungen, Z. Phys. Chem. **57A** (1906) 385–470.

[22] M.J. Temkin, V. Pyzhev, Recent modifications to Langmuir isotherms, Acta Physchim. USSR **12** (1940) 217––222.

[23] O. Redlich, D.L. Peterson, A useful adsorption isotherm, J. Phys. Chem. **63** (1959) 1024.

[24] Y.S. Ho, C.C. Wang, sorption equilibrium of mercury onto ground-up tree fern, J. Hazard. Mater. **156** (2008) 398–404.

[25] S. Lagergren, About the theory of so-called adsorption of soluble substances, K. Sven. Vetenskapsakad. Handl. **24**(4) (1898) 1–39.

[26] Y.S. Ho, G. McKay, Sorption of dye from aqueous solution by peat, Chem. Eng. J. **70** (1998) 115–124.

[27] W.J. Weber, J.C. Morris, Kinetics of adsorption on carbon from solution, J. Sanitary Eng. Division, Am. Soc. Chem. Eng. **89** (1963) 31–59.

[28] M.J.D. Low, Kinetics of chemisorption of gases on solids, Chem. Rev. **60** (1960) 267–312.

[29] G. Alagumuthu, V. Veeraputhiran, M. Rajan, Comments on "Fluoride removal from water using activated and MnO_2-coated Tamarind Fruit (*Tamarindus indica*) shell: Batch and column studies, J.. Hazard. Mater. **183** (2010) 956–957.

[30] N. Viswanathan, S. Meenakshi, Enriched fluoride sorption using alumina/chitosan composite, J. Hazard. Mater. **178** (2010) 226–232.

[31] M.G. Sujana, R.S. Thakur, S.B. Rao, Removal of fluoride from aqueous solution by using alum sludge, J. Colloid Interf. Sci. **206** (1998) 94–101.

[32] I.A.W. Tan, A.L. Ahmad, B.H. Hameed, Adsorption isotherms, kinetics, thermodynamics and desorption studies of 2,4,6-trichlorophenol on oil palm empty fruit bunch-based activated carbon, J. Hazard. Mater. **164** (2009) 473–482.

[33] E. Eren, Removal of copper ions by modified Unye clay, Turkey, J. Hazard. Mater. 159 (2008) 235–244.

[34] M.M. Shihabudeen, S. Atul Kumar, L. Philip, Manganese oxide-coated alumina: a promising sorbent for defluoridation of water, Water Res. **40** (2006) 3497–3506.

IZVOD

SORPCIJA FLUORIDA NA AKTIVNOM UGLJENIKU DOBIJENOM IZ ZUBAČE (*Cynadon dactylon)*

Ganapaty Alagumuthu, Vellaisamy Veeraputhiran, Ramaswamy Venkataraman

Chemistry Research Centre, Sri Paramakalyani College, Tamilnadu, India

(Naučni rad)

U ovom radu proučavana je primena termički aktiviranog ugljenika dobijenog iz biljke zubača (*Cynadon dactylon*) za uklanjanje fluoride iz vode za piće. Adsorpcija je rađena u šaržnim uslovima u neutralnoj sredini u zavisnosti od vremena kontakta, adsorbovane doze, koncentracije adsorbata, temperature i prisutnih anjona. Dobijeni rezultati ukazuju da su adsorbciona mesta na površini adsorbenta heterogenog karaktera i da se mogu opisati modelom heterogenih vezujućih mesta. Dati sistem se pokorava Redlich–Peterson-ovoj kao i Langmuir-ovoj izotermi. Brzina adsorpcije fluorida je modelovana Lagergren-ovim reakcijom pseudo-prvim redom, reakcijom pseudo-drugim redom, difuzijom unutar čestice, i Elovich-ovom kinetikim modelom. Nađeno je da je kinetika adsorpcije pseudo-drugog reda. Izračunate vrednosti standardne promene entalpije i entropije za proces adsorpcije su 8,725 kJ/mol i 0,033 J/mol K, redom, koje ukazuju na to da je proces endoterman. Adsorbat aktivni ugalj je ispitivan rendgenskom strukturnom analizom (XRD), infracrvenom spektroskopijom (FTIR) i skanirajućom elektronskom mikroskopijom (SEM) radi boljeg razumevanja njegove sposobnosti za adsorbciju fluorida.

Ključne reči: Fluoridi • *Cynodon dactylon* • Zubača • Adsorpcija • Izoterme • Kinetički modeli

Key words: Fluorides • *Cynodon dactylon* • Adsorption • Isotherms • Kinetic models